Trajectory Analysis for Manned Spaceflight: Aerodynamic Heating of a Two-Person Lunar-Return Vehicle

Jacob J. Menssen* and John Dec†
Georgia Institute of Technology Space Systems Design Lab, Atlanta, GA, USA, 30332

Design of space vehicles requires an understanding and analysis of the intended trajectories. Numerical integrators that consider the many factors on a spacecraft are essential for this understanding. With the purpose of validating a framework for analysis, a design study on the mass percentage required for thermal protection was carried out on a vehicle that was to travel back from the Moon and reenter Earth's atmosphere. Fourth-order Runge-Kutta was chosen to propagate the differential equations. However, this method alone lacks support for time-independent conditions and changing flight regimes. C++ was used to build a more sophisticated approach that could handle all aspects of the design study and minimize computational time. With the support of historical data for the sizing of the Moon-return vehicle, three designs were chosen with the objective of returning two astronauts and 100 kg of samples from a polar Moon orbit while minimizing the mass of the thermal protection system. The designs varied in their geometry; a 45-degree sphere cone, a 60-degree sphere cone, and a truncated sphere similar to the Orion Crew Module. The Orion Crew Module was used as the systems-level baseline, and resizing was conducted as necessary to correct for the two fewer crew members and different shapes of the vehicle. Flight regimes involved consideration of the Moon's gravity, Earth's rotation, hypersonic aerodynamics, atmospheric conditions, and aerodynamic heating. The findings of the design study were that the truncated sphere required the least massive thermal protection system. This finding is supported by the Orion Crew Module taking the same shape. This approach to trajectory analysis is applicable to any number of situations due to its flexible structure and high modularity, proving to be an effective tool for spaceflight analysis.

I. Nomenclature

C_A	=	force coefficient along the axis of rotational symmetry
C_N	=	force coefficient perpendicular and "up" from the axis of rotational symmetry
C_D	=	drag coefficient
C_L	=	lift coefficient
L/D	=	lift-to-drag ratio
ρ_∞	=	freestream density
V_∞	=	freestream velocity
$\dot{q}_w''$	=	heat flux
TPS	=	thermal protection system
ROC	=	rate of change
r_b	=	base radius
r_n	=	nose radius
μ_E	=	Earth standard gravitational parameter
μ_M	=	Moon standard gravitational parameter
μ_b	=	base latitude
R_E	=	radius of Earth
R_M	=	radius of the Moon
R_{EM}	=	radius from Earth to the Moon
r	=	radial distance from center of Earth

*Undergraduate Researcher, Daniel Guggenheim School of Aerospace Engineering, AIAA Student Member 1860943.
†Professor of the Practice, Daniel Guggenheim School of Aerospace Engineering.

r_{12}	=	vector from body 1 to body 2
h	=	altitude
m	=	mass
A_{ref}	=	reference area
T	=	thrust force
g	=	gravitational acceleration
σ	=	bank angle
ω	=	Earth rotation rate
β	=	ballistic coefficient
V	=	velocity
γ	=	flight path angle (measured negative below local horizon)
Ψ	=	heading angle (measured North from East)
θ	=	longitude
ϕ	=	latitude

II. Introduction

A two-astronaut mission is planned to return to Earth from a Lunar orbit with 100 kg of samples, and design optimization requires minimizing the mass that is used in the thermal protection system. This problem is multifaceted, since Earth reentry is defined by the context of the Lunar return. Furthermore, the shape, size, and mass of the vehicle must also be characterized to generate realistic results. A full investigation of the mission, from the Moon to the end of reentry, is required. Only then can an accurate model of the thermal protection system mass be developed.

III. Simulation Framework

A. Numerical Integration

In flight, there are a large set of differential equations that govern both the trajectory and the aerothermodynamic behavior. These are often unsolvable analytically and require a numerical integrator to propagate the vehicle forward in time. At each time step, a new set of state variables must be calculated as defined by their rate of change. However, adding the change to the previous value lacks fidelity and is very inaccurate [1]. For this reason, Fourth-Order Runge-Kutta (RK4) integration is used to compare the changes at four different time steps and weigh them against each other in order to arrive at a more accurate propagation. Equation (1) shows the procedure for calculating the next y value for some arbitrary system (denoted with a subscript $n+1$) as defined by $\frac{dy}{dt} = f(t, y)$, using timestep dt [1].

$$\begin{aligned}
k_1 &= dt f(t_n, y_n) \\
k_2 &= dt f\left(t_n + \frac{dt}{2},\ y_n + \frac{k_1}{2}\right) \\
k_3 &= dt f\left(t_n + \frac{dt}{2},\ y_n + \frac{k_2}{2}\right) \\
k_4 &= dt f\left(t_n + dt,\ y_n + k_3\right) \\
y_{n+1} &= y_n + \frac{k_1}{6} + \frac{k_2}{3} + \frac{k_3}{3} + \frac{k_4}{6}
\end{aligned} \tag{1}$$

By solving for each state variable over many steps, a series of values represents the trajectory of the vehicle. However, this procedure alone lacks support for things that are not represented by rate of change equations. For this reason, the way RK4 was integrated changed $f(t, y) \rightarrow f(t, y, \text{dependent variables, constants})$ and ran a parallel function that updated the dependent variables based on whatever relationship they might have with the system.

For example, if the parachutes are to release at Mach 0.5, there needs to be a way to change the β of the vehicle. In this case, an if statement can check what the Mach number is at each time step and when the time is right, change the dependent variable associated with β.

Programming this in C++ made changing dependent variables easier since references allowed for direct modification of values. A DiffEqs C++ class was created to streamline the modularity of this approach. With the framework in place, many different types of systems could be fitted to the DiffEqs class structure.

B. Class Structure

After defining a modular DiffEqs class, many aerospace experiments were conducted to improve the ease-of-use for aerospace applications. After the most commonly used equations and analytical demands began to crystalize, another C++ class named SCSimulation (spacecraft simulation) was created as an intuitive and computationally efficient problem solving toolbox. SCSimulation also uses another class that was developed called Freestream, which allows for quick access to a model of Earth's atmospheric properties. The model is a combination of the 1976 US Standard Atmosphere (under 80km geometric altitude) and 1962 US Standard Atmosphere (from 80km to 120km geometric altitude) [2].

The analysis chosen to validate the effectiveness of this aerospace toolbox was a two-person Lunar-return mission with the goal of minimizing the mass of the TPS. Four experiments were conducted and the relationship that these experiments have with the C++ classes are shown in Fig. 1.

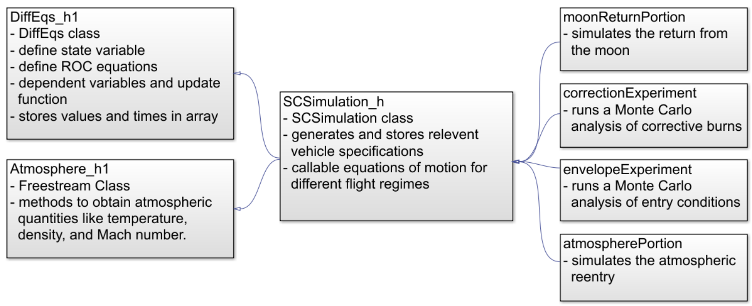

Fig. 1 Diagram showing code structure for spacecraft trajectory experiments.

IV. Trajectory

A. Lunar Return

The starting location of the mission was chosen to be a polar Lunar orbit with an altitude of $100km$. This is due to humanity's interest in the ice located at the Lunar south pole. The orientation of the orbit is such that the angular momentum vector as the spacecraft orbits the moon points away from Earth. This is done so that the engine burn occurs in a tangent direction to the vector from Earth to the Moon, and defines the apoapsis of the return orbit. Using these conditions, a patched conics approximation of the Lunar return was modeled to identify reasonable values of ΔV and time of burn.

Three segments exist for this patched conic approach: the initial circular orbit, the hyperbolic Lunar escape orbit, and the elliptical Earth return orbit. Using properties of elliptical and hyperbolic orbits [3], ΔV and time of burn were approximated.

$$\Delta V = 0.8227 \text{ km/s} \tag{2}$$

$$t_{\text{burn}} = \frac{1000 * \Delta V\, m}{T} \tag{3}$$

1. Equations of Motion

The patched conic approach is a good starting point but the equations of motion of the Earth-Moon systems must be properly characterized for high-fidelity analysis. Acceleration on the Earth and Moon due to the spacecraft was neglected. The acceleration felt by the spacecraft is broken into its Earth and Moon contributions, shown in Eqs. 4-6. The Earth acceleration uses the J_2 model due to its oblateness [4]. The Moon on the other hand is treated as a point mass.

$$\mathbf{a}_E = -\frac{3}{2} J_2 \left(\frac{\mu_E}{r^2}\right)\left(\frac{R_E}{r}\right)^2 \begin{bmatrix} \left(1 - 5\left(\frac{r_z}{r}\right)^2\right)\frac{r_x}{r} \\ \left(1 - 5\left(\frac{r_z}{r}\right)^2\right)\frac{r_y}{r} \\ \left(3 - 5\left(\frac{r_z}{r}\right)^2\right)\frac{r_z}{r} \end{bmatrix} \tag{4}$$

$$\mathbf{a}_M = -\frac{\mu_M}{|r|^3}\begin{bmatrix} r_{ms,x} \\ r_{ms,y} \\ r_{ms,z} \end{bmatrix} \tag{5}$$

$$\mathbf{a} = \mathbf{a}_E + \mathbf{a}_M \tag{6}$$

NASA Horizons [5] was used to generate a file containing the position and velocity of the Moon starting at midnight of March 26th, 2026. These locations were linearly interpolated and used to calculate the radius from the Moon to the spacecraft.

B. Atmospheric Reentry

Once the spacecraft approaches Earth, the atmosphere will be considered to start at $120km$ altitude. At this point the service module is assumed to have separated from the entry vehicle. The equations of motions for atmospheric travel [2] are shown in Eqs. 7-12. These equations are modified to set bank angle and thrust elevation angle to zero since these are not modulated during entry.

$$\frac{dV}{dt} = \frac{T}{m} - \frac{\rho_\infty V^2}{2\beta} - g\sin\gamma + \omega^2 r\cos\phi\,(\sin\gamma\cos\phi - \cos\gamma\sin\phi\sin\psi) \tag{7}$$

$$\frac{d\gamma}{dt} = \frac{V\cos\gamma}{r} + \frac{\rho_\infty V}{2\beta}\left(\frac{L}{D}\right) - \frac{g\cos\gamma}{V} + 2\omega\cos\phi\cos\psi + \frac{\omega^2 r}{V}\cos\phi\,(\cos\gamma\cos\phi + \sin\gamma\sin\phi\sin\psi) \tag{8}$$

$$\frac{d\psi}{dt} = -\frac{V\cos\gamma\cos\psi\tan\phi}{r} + 2\omega\,(\tan\gamma\cos\phi\sin\psi - \sin\phi) - \frac{\omega^2 r}{V\cos\gamma}\sin\phi\cos\phi\cos\psi \tag{9}$$

$$\frac{dh}{dt} = V\sin\gamma \tag{10}$$

$$\frac{d\theta}{dt} = \frac{V\cos\gamma\cos\psi}{r\cos\phi} \tag{11}$$

$$\frac{d\phi}{dt} = \frac{V\cos\gamma\sin\psi}{r} \tag{12}$$

C. Aerodynamic Heating

The Sutton-Graves Correlation [6] was used to approximate the aerodynamic heating of the entry vehicle. This relationship uses a constant K_{Earth} to model the Earth's atmospheric makeup and returns the heat flux at a given moment.

$$K_{Earth} = 1.74153 \times 10^{-4} \tag{13}$$

$$\dot{q}_w'' = K_{Earth}\sqrt{\frac{\rho_\infty}{r_n}}V_\infty^3 \tag{14}$$

Since heat flux is a rate of change, integrating $\dot{q}_w''$ over the trajectory solves for heat load. Heat load is correlated with the TPS mass fraction [7]. This relationship can be approximated using the relationship shown in Fig. 2.

$$\text{TPS Mass Fraction} = 0.091 * (\text{Heat Load})^{0.51575} \tag{15}$$

V. Vehicle Characterization

A critical aspect of analyzing the Lunar-return mission involved the design of a crew vehicle. Historical data was utilized for thrust and mass estimates, while aerodynamic properties depended on geometry. Three entry vehicle geometries were selected for analysis. From least blunt to most blunt, the chosen geometries were a 45-degree sphere cone, a 60-degree sphere cone, and a truncated sphere.

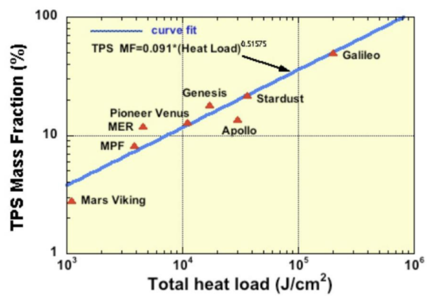

Fig. 2 Historic correlation between heat load and TPS mass fraction. From [7].

The process of sizing these vehicles started with determining the mass and volume necessary for the mission. Since the Orion Crew Module stands as the current state of the art for Lunar-return vehicles, it was used to determine the mass and volume. However, Orion is designed to carry four passengers [8], whereas the mission in question is designed for only two. By reducing the mass and volume of Orion by what is effectively two people's worth of support systems, final estimates were reached. Next, this volume was used to scale historical implementations of each vehicle geometry to the appropriate size. The engines aboard Orion and it's European Service Module were also referenced for thrust estimates.

Hypersonic aerodynamic coefficients for each geometry were calculated using Newtonian Flow. With supporting cross sectional area and mass determined, the ballistic coefficient, β, could be calculated and used in the simulations.

A. Volume

First, a 3D model of the Orion Crew Module was made in SolidWorks. This was done because while the pressurized and habitable volume are published, the total volume is not. The dimensions shown in Fig. 3 were used to create the model, and the volume was found to be $Volume_{Orion} = 30.89m^3$.

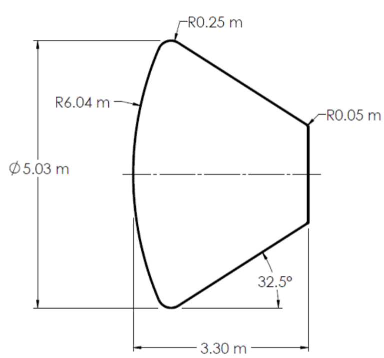

Fig. 3 Geometry of the Orion Crew Module. Adapted from Ref. [9].

With the Orion's total habitable volume published as $Volume_{hab} = 316ft^3 = 8.95m^3$ [8], it was estimated that going from four passengers to two would split this quantity in half. So, the final volume of the desired vehicle can be calculated as shown in Eq. (16).

$$Volume_{final} = Volume_{Orion} - \frac{Volume_{hab}}{2} = 26.42m^3 \tag{16}$$

This volume was then used to size each of the 3 vehicles by scaling their geometries to match the desired $Volume_{final}$.

B. Geometry

The geometry of the 45-degree sphere-cone was based on the Deep Space 2 mission entry vehicle [9]. This geometry was chosen due to it's simple-to-model and volume-maximizing shape. After parameterizing the measurements for this vehicle, it was scaled to match the desired volume. The final dimensions are shown in Fig. 4.

The geometry of the 60-degree sphere-cone was based on the Stardust Sample Return Capsule [9]. This geometry was consistent with other historic 60-degree sphere cones. Using the same process as the 45-degree sphere cone, the desired volume was reached and the final dimensions are shown in Fig. 4.

The geometry of the truncated sphere was based entirely on the Orion Crew Module as shown in Fig. 3. This needed to be scaled as well, and resulted in the dimensions shown in Fig. 4.

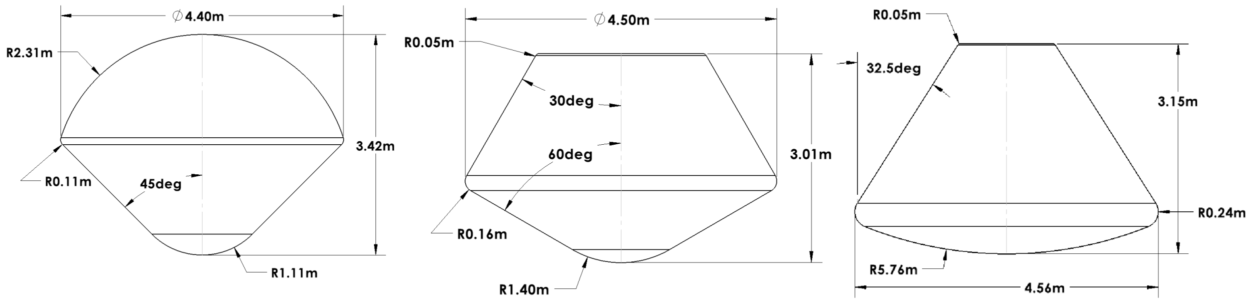

Fig. 4 Dimensions of three scaled entry vehicles for two passengers, designed in SolidWorks. In order of left to right the geometries are 45-degree sphere-cone, 60-degree sphere-cone, and truncated sphere.

C. Mass

Determining mass was done by once again starting with the Artemis Mission as a baseline. The methodology starts by first scaling down appropriate factors with the same ratio as the volume, while leaving non-scalable systems such as payload (100 kg) communications and avionics untouched. A mass breakdown of crew vehicles provided by MIT [10] identifies the total mass percentage of the structural, protection, power, and "other" systems as 58%. See 5.2.3.1.h in [10] for each "other" system. The size of the crew vehicle is 85.45% of the size of Orion. This means that 58% of the mass of Orion is multiplied by 85.45%.

However, passengers have not yet been considered. Equation (17) finds the mass associated with two passengers over the course of a 14 day mission [10].

$$\text{Human Mass} = 2 * (m_{\text{person}} + m_{\text{supplies}} + m_{\text{sleep accom.}} + m_{\text{EVA suits}}) + 2 * 14 * (m_{\text{food}} + m_{\text{clothing}}) = 272.52 \text{ kg} \tag{17}$$

The dry mass estimates of the crew module can then be calculated.

$$m_{\text{CM,dry}} = m_{\text{Orion}} * (0.58 * 0.8545 + 0.42) - 272.52 = 9048.6 \text{ kg} \tag{18}$$

The wet mass is the dry mass scaled by the same proportion of dry and wet masses of Orion [8].

$$m_{\text{CM,wet}} = \frac{m_{\text{Orion, wet}}}{m_{\text{Orion, dry}}} * m_{\text{dry}} = 9229.57 \text{ kg} \tag{19}$$

Lastly, using the proportion between this Orion's mass and its ESM, the same scaling factor will be applied to the crew vehicle to identify its own service module's mass. Before entering the atmosphere this is the vehicle's mass, whereas during entry it is only the crew module.

$$m_{\text{total}} = m_{\text{CM, wet}} + \frac{m_{\text{ESM, wet}}}{m_{\text{Orion, wet}}} * m_{\text{CM, wet}} = 23053.8 \text{ kg} \tag{20}$$

D. Aerodynamics

During Earth reentry the vehicle will be subject to hypersonic flow. At these speeds, Newtonian flow can be used to approximate the coefficients of lift and drag within an acceptable margin [11]. The hypersonic coefficients of lift and drag are needed to quantify the aerodynamic performance of the vehicle during atmospheric reentry. The axial symmetry of entry vehicles leads to these coefficients being functions of the axial and normal force coefficients along with angle of attack.

$$C_L = C_N cos(\alpha) - C_A sin(\alpha) \tag{21}$$

$$C_D = C_N sin(\alpha) + C_A cos(\alpha) \tag{22}$$

The axial and normal coefficients of blunt cones, denoted with subscript bc, are functions of α, r_n, r_b, and δ_c as labeled in Fig. 5.

$$C_{A,bc} = C_{p,max} \left[\frac{1}{2} \left(1 - sin^4(\delta_c) \right) \left(\frac{r_n}{r_b} \right)^2 + \left(sin^2(\delta_c) cos^2(\alpha) + \frac{1}{2} cos^2(\delta_c) sin^2(\alpha) \right) \left(1 - \left(\frac{r_n}{r_b} \right)^2 cos^2(\delta_c) \right) \right] \tag{23}$$

$$C_{N,bc} = C_{p,max} \left(1 - \left(\frac{r_n}{r_b} \right)^2 cos^2(\delta_c) \right) \left(cos^2(\delta_c) sin(\alpha) cos(\alpha) \right) \tag{24}$$

Truncated spheres, denoted with subscript ts, do not have the same parameters as blunted cones and require only the latitude of the cone base, μ_b, in addition to α. μ_b is the angle shown in Fig. 5.

$$C_{A,ts} = \frac{1}{2} sin^2(\alpha) sin^2(\mu_b) + \left(1 + cos^2(\mu_b) \right) cos^2(\alpha) \tag{25}$$

$$C_{N,ts} = sin(\alpha) cos(\alpha) sin^2(\mu_b) \tag{26}$$

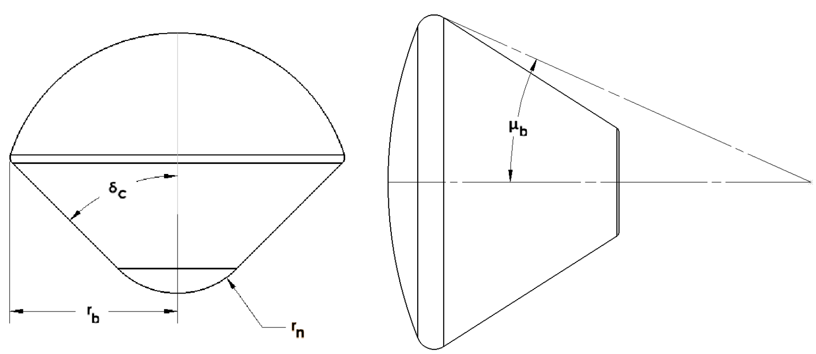

Fig. 5 Relevant geometry of sphere-cone (left) and truncated sphere (right) for hypersonic aerodynamic calculations.

Since angle of attack is to be varied in the experimentation, the final lift and drag coefficients cannot be reported at this stage. However, the other features were determined in the Geometry section. These are shown in Table. 1.

Table 1 Entry Vehicle Features for Aerodynamic Calculations.

Vehicle	Feature	Value
45-degree sphere cone	δ_c	45 deg
	r_b	2.22 m
	r_n	1.11 m
60-degree sphere cone	δ_c	60 deg
	r_b	2.31 m
	r_n	1.40 m
Truncated sphere	μ_b	24.55 deg

The majority of aerodynamic heating occurs at hypersonic Mach numbers. With this in mind, C_L and C_D are assumed to be the values calculated in this section during the entire supersonic regime. This simplification is made because this study prioritizes aerodynamic heating and high speed dynamics to low speed trajectory accuracy. Furthermore, the margin of acceptable trajectory error is very large due to the landing site being the Pacific Ocean.

E. Parachutes

A simplified model of a parachute system is implemented for the same reason that the low-Mach C_L and C_D are not calculated at a high accuracy. That is because low speed aerodynamics are not the important aspect of analysis for this mission. Nonetheless, the simplified model allows for a much better estimate of touchdown location than no parachute model at all.

The parachute system is modeled as a combination of drogue and main parachutes. The drogue parachutes will deploy at Mach 1 and the main parachutes will deploy at Mach 0.5.

Using NASA publications [12], the drogue (subscript d) and main (subscript m) parachutes aboard Orion can be characterized with Eqs. (27)-(30). Note that there are two drogue parachutes and three main parachutes, adding the respective multiplier to the reference area.

$$C_{D,b} = 0.52 \tag{27}$$

$$A_{ref,d} = 18.37 * 2 = 36.75 \text{ m}^2 \tag{28}$$

$$C_{D,m} = 1.75 \tag{29}$$

$$A_{ref,m} = 466.93 * 3 = 1400.79 \text{ m}^2 \tag{30}$$

F. Engines

The engines aboard this vehicle are taken to be functionally identical to those used in the Artemis I mission, including both the European Service Module (ESM) and the Orion Crew Module [13]. There are three propulsion systems of interest.

The main engine on the ESM is the Orbital Maneuvering System Engine. This engine is capable of 26689.3 N of force [13]. This engine will be utilized in the mission to escape from the Lunar sphere of influence and begin the transfer orbit back to Earth.

The Auxiliary Engines on the ESM are for trajectory corrections [13], which is how they will be incorporated into this mission. Providing 444.822 N of thrust, they will allow for corrective maneuvers as necessary to ensure a safe return to Earth.

Lastly, the Reaction Control System Engines on the Orion Crew Module are for orientation upon separation from the ESM and entry into Earth's atmosphere [13]. These are not quantified numerically in this analysis, and are instead assumed to maintain the commanded angle of attack during reentry.

VI. Results

A. Return Trajectory

The ΔV, as defined by Eq. (2), was planned to be 0.8227 km/s. This number had to be changed slightly to 0.937 km/s due to inaccuracies in the patched conics model. This burn was timed such that the spacecraft escaped its Lunar orbit in a near-equatorial plane. This trajectory simulation was stopped when the spacecraft was 100,000 km from Earth's surface and plotted in Fig. 6.

The next step was to conduct a corrective maneuver with a small burn. This was to allow for a choice in γ. Data for this burn was gathered by running the simulation from the most recent point 20 times and varying ΔV slightly. The results are shown in Fig. 7

B. Vehicle Selection

To identify the vehicle with the lowest TPS mass fraction, the entry profile had to be understood first. A Monte Carlo simulation tested 1600 potential combinations of α and γ and plotted their TPS mass percentage after reentry. Fig. 8, Fig. 9, and Fig. 10 show the results for each vehicle. Blacked-out data-points are where the acceleration exceeds 9 G, and would be fatal to human passengers. The highlighted "best" data point is the lowest possible TPS mass fraction in the survivable region. The truncated sphere has the best result, with a TPS mass percentage of 14.65%, making it the winning candidate. This result aligns with the Orion Crew Module taking the same shape.

Finally, the Earth reentry was ready to be simulated. A corrective burn of $\Delta V = 0.17$ km/s $\Rightarrow \gamma = -6.13$ deg was made with a commanded $\alpha = -3.52$ deg during entry. Note that these angles are moved 0.1 degree into the "safe" region. The crew module touched down in the Pacific Ocean at latitude 5.74 North and longitude 148.44 East. The final TPS mass makeup was 15.19%.

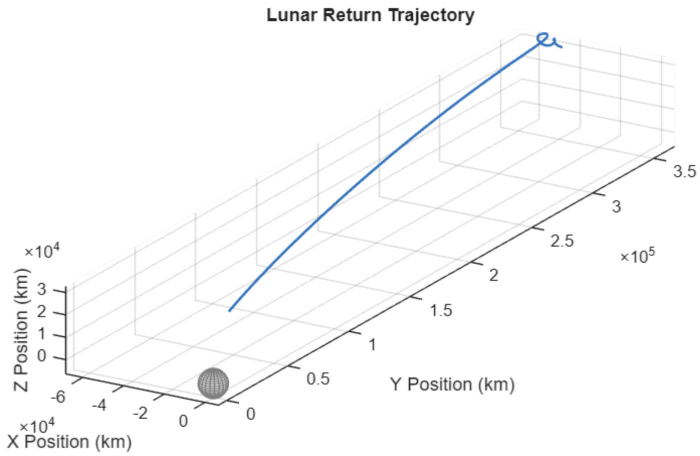

Fig. 6 Trajectory of spacecraft as it makes an orbit around the Moon then burns to begin it's return orbit to Earth, ending 100,000 km away from the Earth's surface

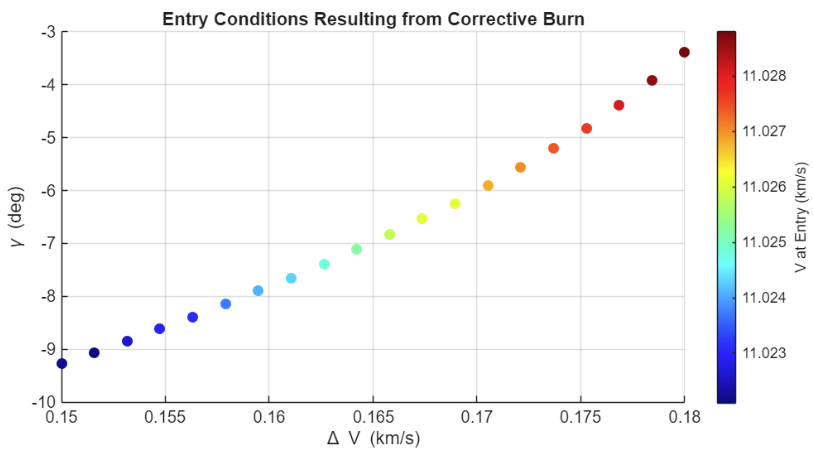

Fig. 7 Flight path angle and velocity at entry as a function of ΔV used in corrective maneuver.

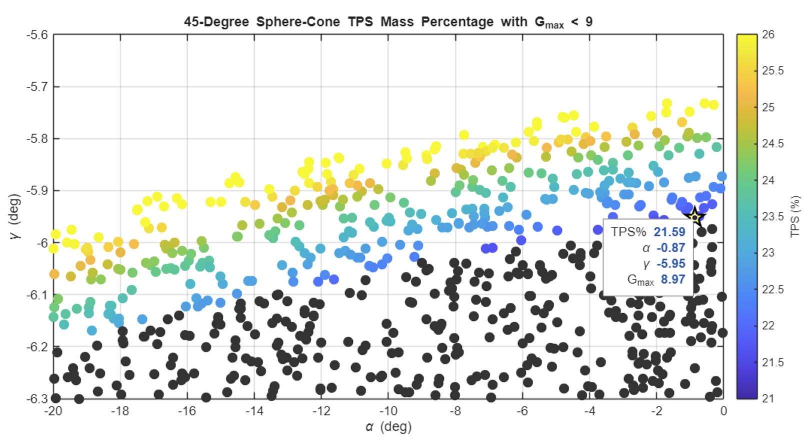

Fig. 8 Results of 45-degree sphere-cone Monte Carlo simulation for entry into Earth's atmosphere. TPS mass percentage is represented in color for non-lethal (G_{max} < 9) entries, with the lowest marked.

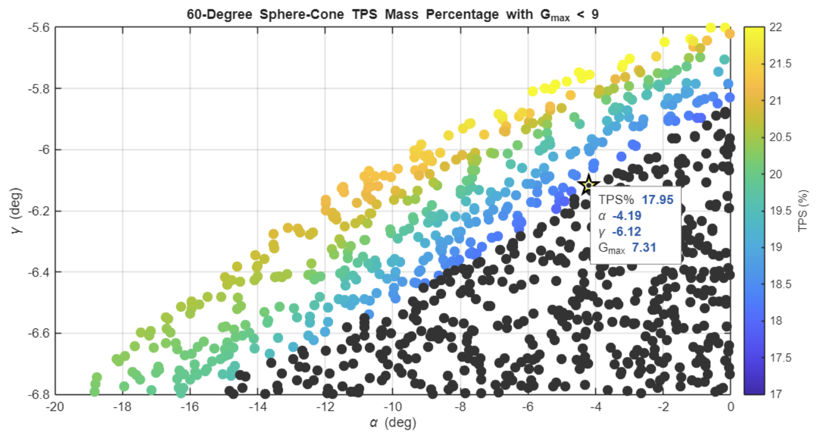

Fig. 9 Results of 60-degree sphere-cone Monte Carlo simulation for entry into Earth's atmosphere. TPS mass percentage is represented in color for non-lethal ($G_{max} < 9$) entries, with the lowest marked.

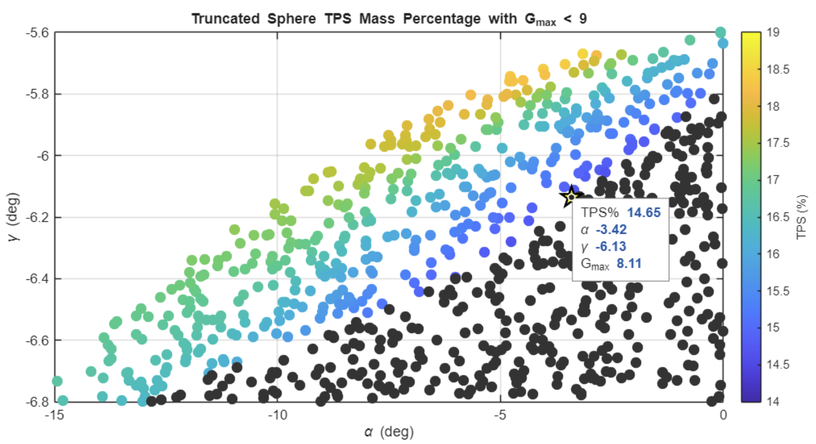

Fig. 10 Results of truncated sphere Monte Carlo simulation for entry into Earth's atmosphere. TPS mass percentage is represented in color for non-lethal ($G_{max} < 9$) entries, with the lowest marked.

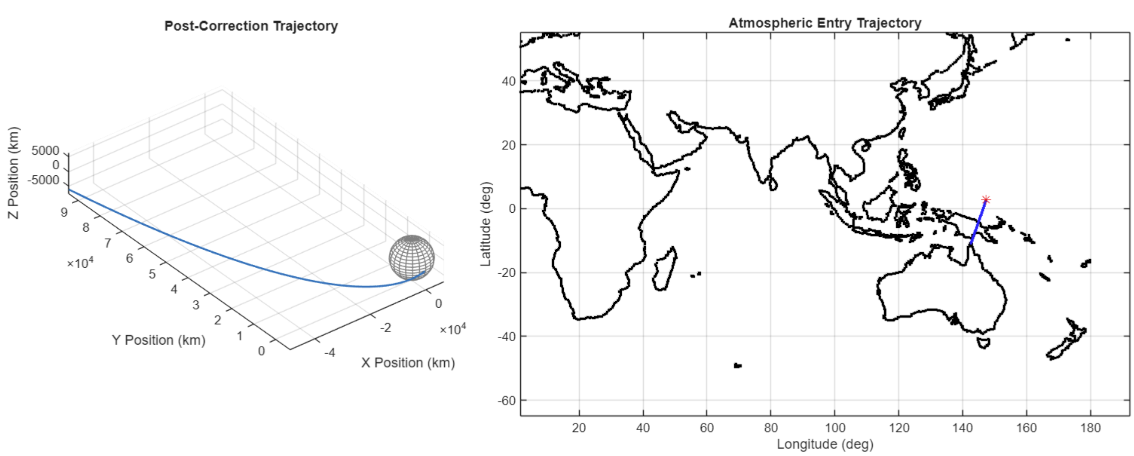

Fig. 11 Trajectory of truncated sphere crew module after a 0.17 km/s ΔV corrective maneuver with reentry and touchdown.

VII. Conclusion

Using a combination of historical data and a custom numerical integration platform, a successful analysis of entry vehicle aerodynamic heating was conducted. Truncated spheres exhibit the best TPS mass percentage for this mission, and exhibited a survivable entry envelope. This study could be expanded to non-human cargo for further analysis beyond $G_{max} = 9$. Additionally, the spacecraft simulation software is an extremely useful and customizable tool that can be applied to any number of situations. Studies like these inform how powerful tools can work alongside engineering methodology to arrive at actionable results.

References

[1] Press, W. H., Teukolsky, S. A., Vetterling, W. T., and Flannery, B. P., *Numerical Recipes in C++: The Art of Scientific Computing*, 2nd ed., Cambridge University Press, New York, NY, USA, 2002.

[2] Regan, F. J., and Anandakrishnan, S. M., *Dynamics of Atmospheric Re-Entry*, Progress in Astronautics and Aeronautics, Vol. 123, American Institute of Aeronautics and Astronautics, Washington, DC, 1993.

[3] Bate, R. R., Mueller, D. D., and White, J. E., *Fundamentals of Astrodynamics*, Dover Books on Aeronautical Engineering, Dover Publications, New York, NY, 1971.

[4] Curtis, H. D., *Orbital Mechanics for Engineering Students*, 3rd ed., Elsevier, 2014.

[5] NASA Jet Propulsion Laboratory, "HORIZONS System," `https://ssd.jpl.nasa.gov/horizons/`, 2026. Accessed 26 February 2026.

[6] Sutton, K., and Graves, J., Robert A., "A General Stagnation-Point Convective Heating Equation for Arbitrary Gas Mixtures," Tech. Rep. NASA TR R-376, NASA, Washington, DC, 1971.

[7] Laub, B., and Venkatapathy, E., "Thermal Protection System Technology and Facility Needs for Demanding Future Planetary Missions," *International Workshop on Planetary Probe Atmospheric Entry and Descent Trajectory Analysis and Science*, Lisbon, Portugal, 2003.

[8] National Aeronautics and Space Administration, "Orion by the Numbers," `https://www.nasa.gov/wp-content/uploads/2015/06/fs-2014-08-004-jsc-orion_quickfacts-web.pdf?emrc=90e48d`, 2022. Infographic. Accessed 26 February 2026.

[9] Hash, D. B., Parcero, K., Allen, G., Witkowski, A., McKee, S., Torres, L., and Davies, C., "Planetary Mission Entry Vehicles Quick Reference Guide, Version 4.1," Special Publication NASA SP-20230010341, NASA, Washington, DC, 2023. URL `https://www.nasa.gov/wp-content/uploads/2023/08/final-planetary-mission-entry-vehicles-quick-reference-guide-v4.1-.pdf`, accessed 26 February 2026.

[10] National Aeronautics and Space Administration, "Exploration Systems Architecture Study (ESAS): Final Report," Tech. Rep. NASA-TM-2005-214062, NASA, Washington, DC, 2005. URL `https://ocw.mit.edu/courses/16-423j-aerospace-biomedical-and-life-support-engineering-spring-2006/4f4e9b34efc79da57336b501ccc8f31f_esas_report_02_2.pdf`, accessed 26 February 2026.

[11] Heybey, W. H., "Newtonian Aerodynamics for General Body Shapes with Several Applications," Technical Note NASA TN D-3984, NASA, Washington, DC, 1967.

[12] Ray, E. S., "Low-Speed Flight Dynamic Tests and Analysis of the Orion Crew Module Drogue Parachute System," Technical Memorandum NASA/TM-2008-215198, NASA, Hampton, VA, 2008. URL `https://ntrs.nasa.gov/api/citations/20080033127/downloads/20080033127.pdf`, accessed 26 February 2026.

[13] National Aeronautics and Space Administration, "Fired Up: Engines and Motors Put Artemis Mission in Motion," `https://www.nasa.gov/missions/artemis/orion/fired-up-engines-and-motors-put-artemis-mission-in-motion/`, 2022. Accessed 26 February 2026.